Residual and thermal strain in AX41 magnesium alloy reinforced with short Saffil fibres

A. Rudajevová, K. Milička

Residual and thermal strain in AX41 magnesium alloy reinforced with short Saffil fibres

A. Rudajevová, K. Milička

PII: S0266-3538(08)00177-2
DOI: 10.1016/j.compscitech.2008.04.034
Reference: CSTE 4067

To appear in: *Composites Science and Technology*

Received Date: 11 December 2007
Revised Date: 15 April 2008
Accepted Date: 26 April 2008

Please cite this article as: Rudajevová, A., Milička, K., Residual and thermal strain in AX41 magnesium alloy reinforced with short Saffil fibres, *Composites Science and Technology* (2008), doi: 10.1016/j.compscitech.2008.04.034

Residual and thermal strain in AX41 magnesium alloy reinforced with short Saffil fibres

A. Rudajevová, K Milička*

Charles University, Faculty of Mathematics and Physics, Department of Condensed Matter Physics, Ke Karlovu 5, 121 16 Praha 2, Czech Republic,

**Institute of Physics of Materials, Academy of Sciences of Czech Republic, Žižkova 22, 616 62 Brno, Czech Republic*

Abstract

Thermal expansion characteristics of AX41 magnesium alloy reinforced by 12 vol. % of short Saffil fibers were investigated at the temperature range of 25 to 380 ºC. Specimens cut at various angles involving random planar distribution of fibers were used for the experiments. From the thermal expansion characteristics, residual and thermal strains and their dependence on the orientation were evaluated. Tensile thermal strains were observed from 0° to 45° angles between the axis sample and the preferential plane of the fiber distribution. For greater angles, i.e., 45°–90º, the compression thermal strains were observed. The thermal stresses and the thermal strain connected with them head towards stress-free state by elastic-plastic mechanism. The temperature of the elastic-plastic transition does not depend on the angle between sample axis and the short fiber direction.

Keywords: A. Metal-matrix composites, Short – fiber composites; B. Thermal properties; C. Stress relaxation

1. Introduction

Metal matrix composites reinforced by short ceramic fibers represent typical systems of phases with different coefficients of thermal expansion (CTE). Because of these differences, local strains occur inside these materials in the matrix as well as in the reinforcement. In principle, two types of the macroscopic strains can be distinguished in the composite. First, residual strains are a consequence of material preparation, e.g., mechanical procedures, and as a rule, can be simply removed by heating. The nature of these strains is usually tensile [1,2]. Residual strains can also be introduced any time by additional deformation of the sample. Second, the thermal strains are attributes of the system in any state and can be assigned exclusively to differences in CTE of phases. These strains cannot be removed by any process from the composite because they occur during cooling and they release during heating. Releasing of the thermal strains takes place by the elastic-plastic mechanism [1].

During fabrication cooling, the composite goes through the so-called stress-free state where no internal stresses exist in a composite material. The flow stress of the metallic matrix is usually very low so plastic deformation of the matrix occurs during cooling almost instantaneously. This plastic deformation begins within the first few degrees of cooling. Levy et al. [3] have shown on Al alloy/SiC composite that plastic deformation finishes at about 225 ºC. No plastic deformation occurs between 225 and 65 ºC. In this paper FEM-simulation were made with assumption one direction ordering of fibres in the matrix and the material was cooled from 500 ^{o}C to room temperature. Thermal plastic deformation disappeared due to the temperature dependence of the yield strength of the matrix alloy. Plastic deformation in the composite is localized in the matrix near the interface between matrix/reinforcement. This region of the matrix can produce complex effects on the composite responses during its mechanical loading. It has

been reported that the thermal stresses can result in asymmetric stress-strain responses under tensile and compressive loading [4,5,6].

Both types of the local strains have been detected by several experimental procedures such as X-ray diffraction [7] and dilatation techniques [8]. In the latter, the measured coefficient of thermal expansion of a given material includes the changes not only in atom vibrations but also in all deformations with temperature. Therefore, measurements of CTE can serve well in identifying the integral changes in local strains.

The distribution of reinforcing fibers in metal matrix composites is usually not regular; their arrangement strongly depends on the procedure of fabrication of the composite. The present paper consists of an investigation of the influence of the specific arrangement on directional dilatation characteristics of a composite with a magnesium alloy AX41 matrix with short ceramic Saffil fibers in a wide temperature interval from 25 to 380 ºC.

2. Experimental details

The materials for the present study were magnesium composites based on AX41 (Mg-4Al-1Ca) alloy, which was reinforced by 12 vol. % Saffil fibers. The composites were supplied by the Centre of Advanced Materials, Clausthal, and were prepared by squeeze casting. The molten alloy (700 ºC) was inserted into a preheated die (350 ºC) with Saffil preform. The two-stage application of pressure was used (40 MPa for 15 s followed under 70 MPa for 90 s). The ingot dimensions were 100 x 100 x 30 mm.

Short fibers in the composite held their original arrangement existing in the preform; they were planar randomly arranged, i.e., axes of fibers lay randomly in parallel planes xy (Fig. 1). The length of the fibers was in order of tens of μm and their diameter (thickness) approximately 3 μm. Particles of secondary phases, namely, $CaAl_2$, were

randomly distributed in the structure. From the composite part of the ingot, parallelepipeds, which contain different angles α with preferential plane xy of the fiber distribution (Fig. 1), were cut. Cylindrical specimens of 6 mm in diameter and 25 mm or 20 mm long were prepared for dilatation measurements. The composite samples with angle α= 0, 30, 45, 60 and 90 ˚ are further called C-0, C-30, C-45, C-60 and C-90.

The linear thermal expansion of the composite specimens was measured in a helium atmosphere by using a Netzsch 402 C/4/G dilatometer from room temperature to 380 ºC at heating and cooling rates of 2 ºC/min. The thermal expansion curves for composites were measured during three consequent heating and cooling cycles. In all cases, results obtained in the second thermal cycle were the same as those in the third cycle. Therefore, in the following, dilatation characteristics obtained in the first and second thermal cycles only will be presented and discussed. The first cycle was performed in the as-cast state.

3. Experimental results

The substantial difference between the dilatation characteristics obtained in the first and the second thermal cycles was a permanent reduction of the sample length after the first thermal cycle. The value of the reduction of the sample length was about 25 μm. For a better understanding of the processes occurring in composites during thermal cycling, the measured relative elongation on several contributions can be divided. These contributions were additive. Measured relative elongation $(\Delta l/l_o)_{meas}$ can be expressed as

$$\left(\frac{\Delta l}{l_o}\right)_{meas} = \frac{\Delta l}{l_o} + \left(\frac{\Delta l}{l_o}\right)_{RS} + \left(\frac{\Delta l}{l_o}\right)_{TS} \quad (1)$$

where $\frac{\Delta l}{l_o}$ is the relative elongation caused by thermal vibrations, $\left(\frac{\Delta l}{l_o}\right)_{RS}$ is the residual strain, and $\left(\frac{\Delta l}{l_o}\right)_{TS}$ is the thermal strain. Term $\frac{\Delta l}{l_o}$ can be determined by the rule of mixtures and it increases with increasing temperature ($(CTE)_{Saffil}$= 7.6 10^{-6} K^{-1}, $(CTE)_{AX41}$= 24.9 10^{-6} K^{-1}). The residual strain for all composites as well as for pure alloy AX41 is shown in Figure 2. The residual strain was obtained as the difference between the first and second thermal cycles.

Figure 3 shows the temperature dependence of the relative elongation for all composites in the second thermal cycle. Dilatation depends on the architecture of the short fiber arrangement concerning the axis of the sample. Figure 4 reveals temperature dependence of the CTE for heating part of the thermal cycle. Figure 5 shows the same dependences for cooling. The character of these dependences was different for various orientations during heating but the same during cooling. The CTE moderately increased with increasing angle. Relation (1) can be used in calculating the thermal strain when term $\Delta l/l_o$ is substituted by the values obtained from the rule of mixtures. If the relative elongation is used and measured in the second thermal cycle, the thermal strain values will be obtained. Temperature dependences of the thermal strain for all composites studied are shown in Figure 6. Obviously, the thermal strain strongly depended on the orientation of the fiber to the axis of the sample. Scheme of the thermal strain components at angle α and dependence of the measured values of the thermal strain on angle α is presented in Figure 7.

Figure 8 reveals the temperature dependence of the residual strain that occurred in the composite when various cooling rates were used. The composite C-0 was used for this experiment. The composite was heated 24 h at 400 ^{o}C (this temperature was used for the

heat treatment) and then it was quenched in air, water, and liquid nitrogen. The dilatation characteristics were then measured during two thermal cycles. The residual strain was calculated from relation (1). Figure 8 shows that character of the residual strain after quenching was different from the residual strain that occurred during preparation of the composite.

4. Discussion

The dilatation characteristics of the AX41 alloy had a standard course. After the first thermal cycle, a reduction of the sample length occurred. The residual strain was released only during heating. Figure 2 shows that the residual strain in the alloy was practically the same as the residual strain in the composites. The temperature dependence of the relative elongation and the CTE in the second and the third thermal cycles were the same. No hysteresis was found during heating and cooling. It is necessary to note that the alloy sample was prepared from the same ingot as composites studied.

The residual strain in the composites was found only in the as-prepared composites. Figure 2 shows the release of the residual strain that was not practically dependent on the direction of the fibers to the axes of the sample. The results reveal that the alloy and the matrix of the composite in as-prepared state were always in tension (after the first thermal cycle reduction of the sample length occurs). This effect is evidently connected with solidification when the volume of the solid is lower than the volume of the liquid. The temperature gradient in the ingot during cooling decreased from the ingot center to its margin. So the margin of the ingot solidified first. The interior of the ingot cannot reduce its volume and the composite is therefore deformed in tension. This tensile deformation is then removed in the following thermal cycle. Amount of this removed deformation depends on the maximum thermal cycle temperature and on the heating rate.

The thermal strain occurred in the composite as consequence of the difference of the CTE of the alloy and reinforcement during cooling. The existence of the thermal strain in composites was connected with the hysteresis on the temperature dependence of the relative elongation. This means that the development and release of the thermal strain did not occur in the same manner (Fig. 3). Similar results were presented by Kumar et al. in the works [9,10] on the Mg fiber composites. The hysteresis and the residual strain were found in their work for transversal and perpendicular orientation of the fibers to the sample axis.

The temperature dependence of the CTE during heating for all composites studied is shown in Figure 4. On each curve were linear section and section where curvature occurred above 220 ºC. This curvature was connected with the decrease in the CTE for C-0 and C-30 composite and increase in CTE for C-90, C-60, and C-45 composites. These departures from the linear dependence mean that the relative elongation was caused by thermal vibration and some further deformation. If the CTE increased as in the case of C-90 and C-60, then deformation was positive and the sample length increased during heating; the sample was in compression deformation before heating. On the other hand, when the temperature dependence of the CTE was curveted to lower values of the CTE, the sample was in tensile deformation and during heating the sample length would be reduced when tensile deformation was released. In a previous work [11], the CTE of the predeformed composite in compression increased and it decreased when the composite was predeformed in tension.

During cooling of composite, thermal stresses can be introduced into each constituent because of a high thermal mismatch between a ceramic reinforcement and a metal matrix. The linear thermal mismatch strain resulting from a temperature variation ΔT is often published as [12]

$$\varepsilon_{th} = (\alpha_M - \alpha_F)\Delta T \quad (2)$$

where α_M is the matrix coefficient of thermal expansion and α_F is the inclusion coefficient of thermal expansion. Term ΔT is the difference between T_o, that is temperature where the stress-free state exists, and actual temperature T. It was evident that the thermal mismatch strain was highest at lowest temperature; it decreased with increasing temperature and reached zero at the stress-free state. The thermal stresses and the thermal strain in the components connected with them depended on other factors such as the size and shape of inclusions and the character of the interface. For example, Yih and Chung [13] have shown that the composite reinforced with the Cu-coated SiC whisker had a lower linear CTE than that of the corresponding composites with the uncoated one. The thermal strain in the composite was determined by the character and by the density of the dislocations in metal matrix near the interface between the matrix and reinforcement.

Anisotropy of the thermal strain was perceptible from all the results (Fig. 1-6). With regard to the results obtained for C-0 and C-90 composites, during heating, the thermal stress in the composite decreased at first only elastically. When the thermal stress reached the yield stress of the matrix, at a certain (high) temperature, plastic zones near the interfaces between the matrix and fibers were reduced (yield stress decreases with increasing temperature). The elastic stress field was modulated by this plastic deformation and decrease (C-0) or increase (C-90) in the thermal strain was faster than in the case of only the elastic deformation range. The temperature boundary between elastic and elastic-plastic mechanism may be defined as bend on the temperature dependence of the CTE during heating (Fig. 4). The transient temperature is about 220 ºC. It is assumed that the matrix is strained in tension in the direction parallel to the fiber planes. The decrease in the thermal stress (strain) in this direction is then associated with the

197 reduction of the specimen length ($\left(\frac{\Delta l}{l_0}\right)_{TS}$ <0). On the other hand, the matrix is deformed
198 in compression in the direction perpendicular to the fiber planes. The decreasing thermal
199 stress (strain) leads to an expansion of the specimen length in this direction ($\left(\frac{\Delta l}{l_o}\right)_{TS}$ >0).
200 The yield stresses for heating and cooling do not coincide so that hysteresis is observed.

201 The C-45 composite has practically zero thermal strain (Fig. 6). The composites C-
202 30 and C-60 behave similarly as the composites C-90 and C-0; only the values of the
203 thermal strain are lower in the entire temperature range studied. The plastic zones
204 disappear at about 220 ºC, the bend on the temperature dependence of the CTE occurs at
205 about this temperature. The scheme of the thermal strain components at angle α and
206 dependence of the measured values of the thermal strain on angle α is shown in Figure 7.
207 The highest thermal strain is in the direction of the fibers and in the direction
208 perpendicular to a planar random arrangement.

209 Figure 8 reveals the temperature dependence of the residual strain that has occurred
210 by the quenching of C-0 composite from 400 ºC up to air, water, and liquid nitrogen.
211 Release of this residual strain has not the same course as in the case the residual strain
212 that occurred because of manufacturing cooling. Substantial difference is perceptible on
213 dependence of the residual strain that was obtained by the quenching in liquid nitrogen.
214 This quenching of the composite C-0 into liquid nitrogen leads to compression
215 macroscopic deformation in the fibers' direction. Release of the residual strain during
216 heating is connected with an increase of above 200 ºC. This effect was not found during
217 release of the manufacturing thermal strain and is not probably connected with
218 precipitation because heating of the pure alloy and its quenching into liquid nitrogen do
219 not change the dilatation characteristics.
220

5. Conclusions

The residual strain was found in all as-prepared samples of the composites and the pure alloy. This residual strain was tensile in all cases and it was not dependent on the place of the sample in the ingot. The residual strain occurs also during quenching of the composite from a high temperature up to air, water, or liquid nitrogen. This residual strain, however, has different character from the residual strain after manufacturing cooling. The thermal strain depends on direction of the short fibers to the sample axis. In direction where angle of the sample axis and fibers is 45º, zero thermal strain exists. The highest thermal strain was found for side angles; compression for the case when the axes of the sample was perpendicular to the place of a planar randomly arranged short fibers, and tensile when the axis of the sample was parallel to the fibers. Increasing temperature leads to release of the thermal strain. The sample length increases/decreases when the compression/tensile strain is released. This process has elastic-plastic character. At low temperatures, below 220 ºC, the thermal strain relaxation has only elastic character. Above this temperature the plastic zones in the matrix near fibers disappear and this process accelerated relaxation of the thermal strain.

Acknowledgments

The authors are grateful for the support offered by the Grant Agency of the Czech Republic under Grant 106/06/1354. This work is also a part of the research program MSM 0021620834 that is financed by the Ministry of Education of the Czech Republic.

References

[1] Rudajevová A, Lukáč P. Acta Mater 2003;51:5579.

[2] Arsenault RJ, Taya M. Acta Mater 1987;96:77.

[3] Levy A, Papazian JM. Acta Metall Mater 1991;39:2255.

[4] Dutta I, Sims JD, Seigenthaler DM. Acta Metall Mater 1993;41:885.

[5] Shi N, Wilner B, Arsenault RJ. Acta Metall Mater 1992;40:2841.

[6] You JH, Bolt H. J Nuclear Mater 2002;307:74.

[7] Mari D, Krawitz AD, Richardson JW, Benoit W. Mater Sci Eng 1996;A209:197.

[8] Rudajevová A, Lukáč P, Kudela S, Kudela S. Scripta Mater 2005;53:1417.

[9] Kumar S, Mondal AK, Dieringa H, Kainer KU. Comp Sci Technol 2003;63:1805.

[10] Kumar S, Ingole S, Dieringa H, Kainer KU. Comp Sci Technol 2004;64:1179.

[11] Rudajevová A, Padalka O. Comp Sci Technol 2005;65:989.

[12] Dunand D, Mortensen A, Mater Sci Eng 1991;135:79.

[13] Yih P, Chung DDL. J Mater Sci 1996;31:399.

[14] Huang YD, Hort N, Kainer KU. Composites A 2004;35: 249.

List of captions

Fig. 1 – Scheme of composite ingot and manner of cutting of samples (a), illustration of random planar distribution of fibers in the composite (b).

Fig. 2 – Temperature dependence of the residual Fig strain in as-prepared samples

Fig. 3 - Temperature dependence of the relative elongation of the second thermal cycles

Fig. 4 – Temperature dependence of the CTE for heating in the second thermal cycles

Fig. 5 - Temperature dependence of the CTE for cooling in the second thermal cycles

Fig. 6 – Temperature dependence of the thermal strain in the second thermal cycles

Fig. 7 – Schema of the thermal strain components at angle α (a) and dependence of the measured values of the thermal strain on angle α (b), ε_T and ε_C are tensile and compression deformation

Fig. 8 – Temperature dependence of the residual strain in quenched samples

289

290 Fig.1

291

292

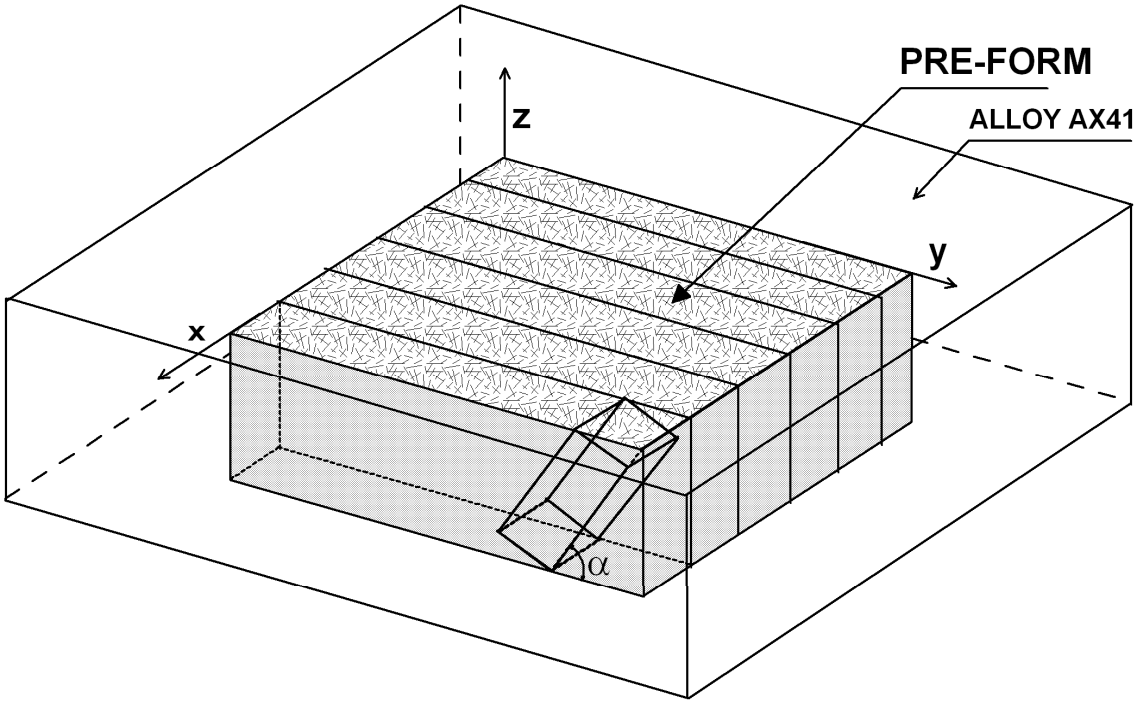

293

294

295 Fig.2

296

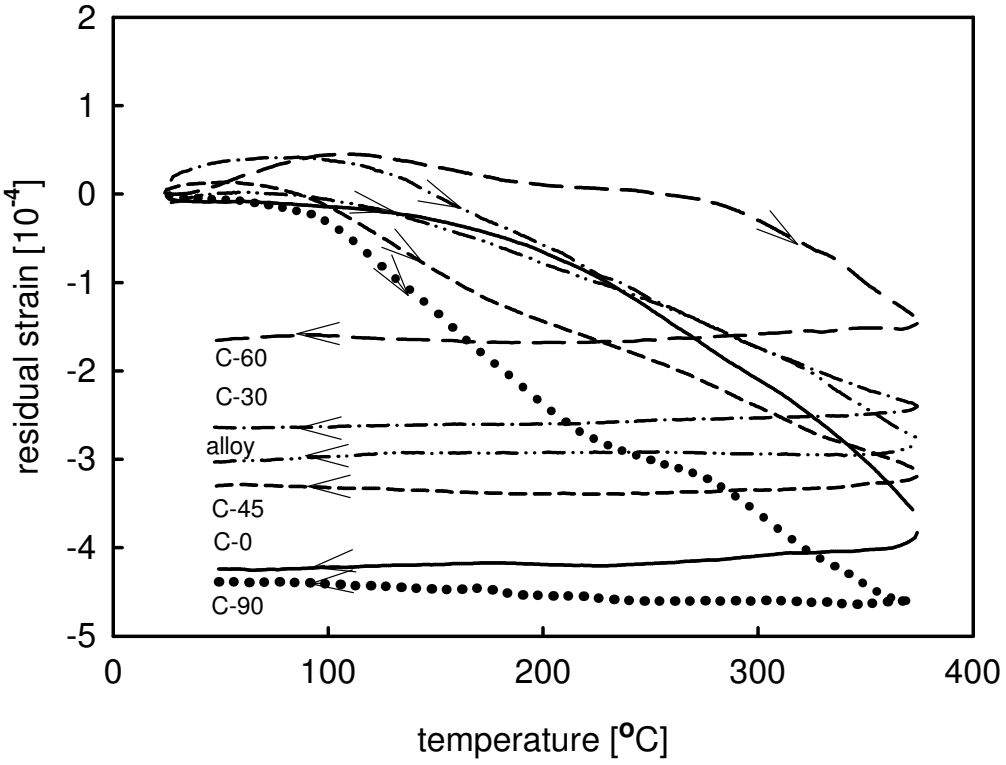

297 Fig. 2 Rudajevova

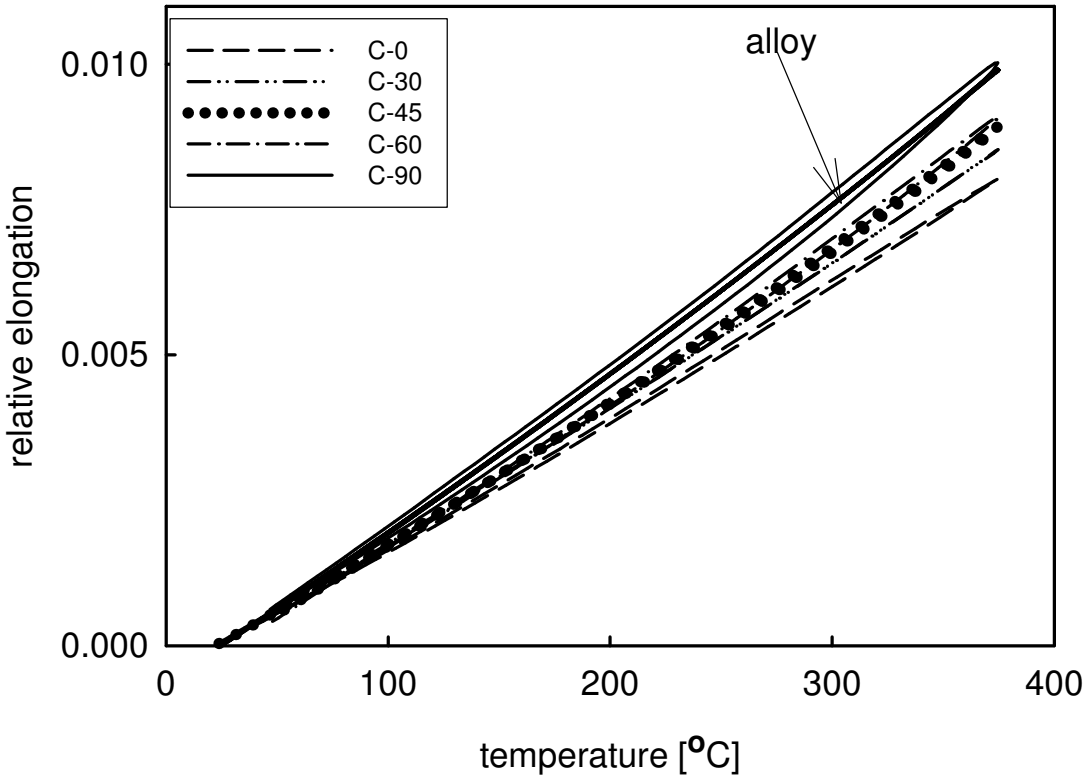

298 Fig. 3 - Rudajevova

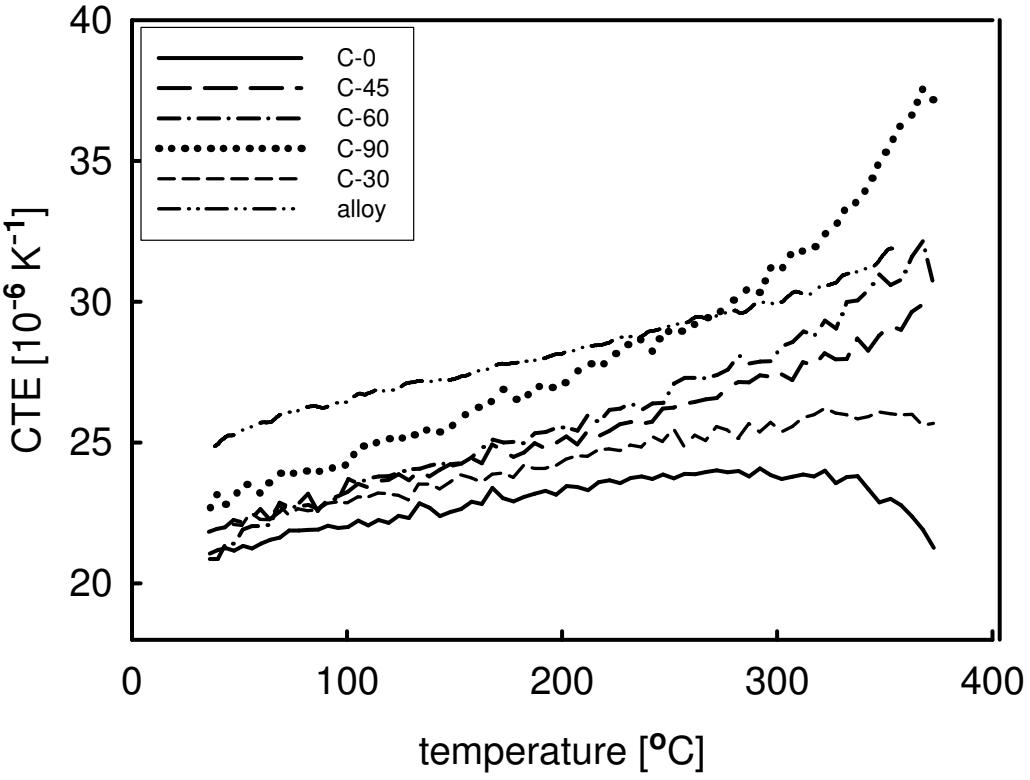

299 Fig. 4 - Rudajevova

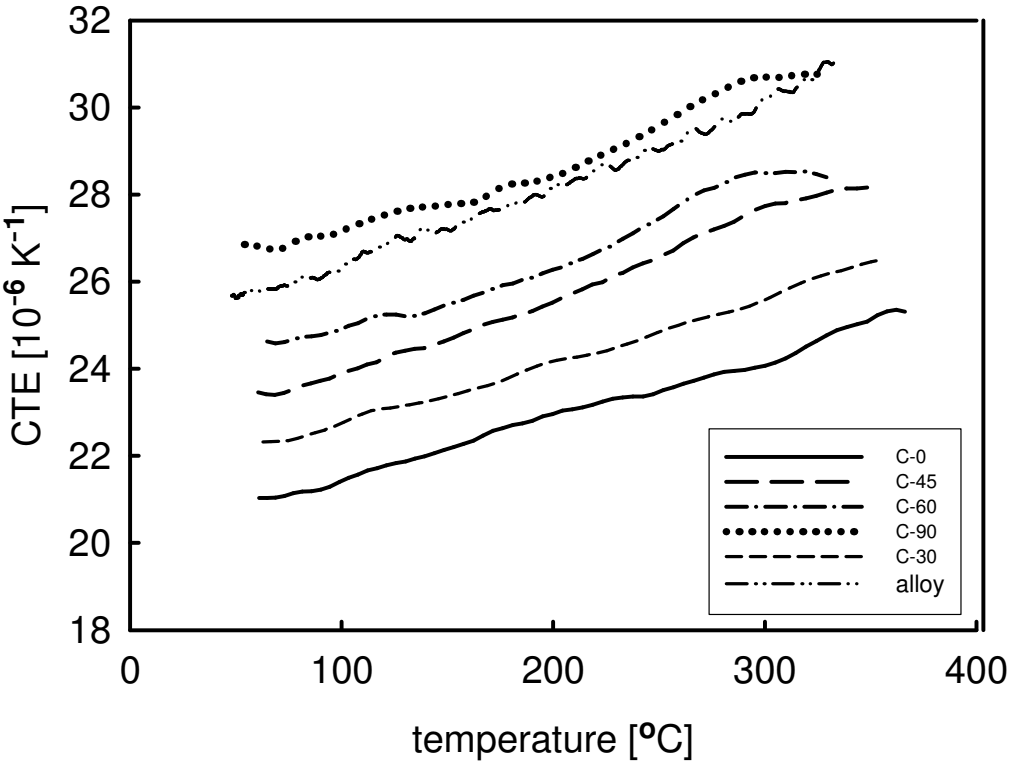

300 Fig. 5 -Rudajevova

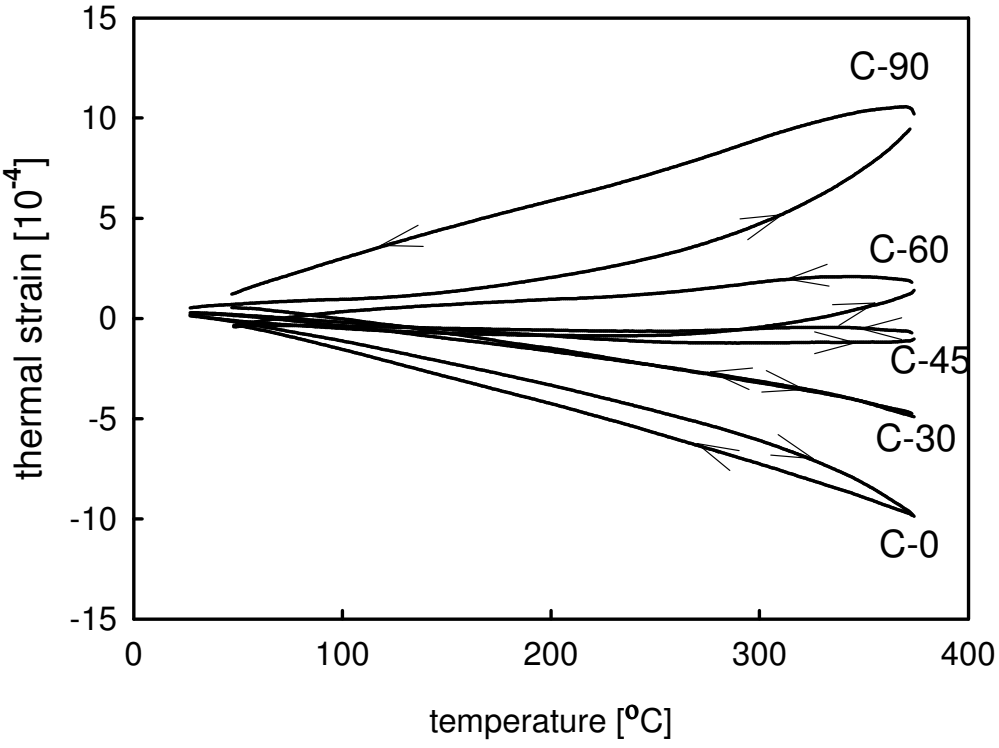

301 Fig. 6 - Rudajevova

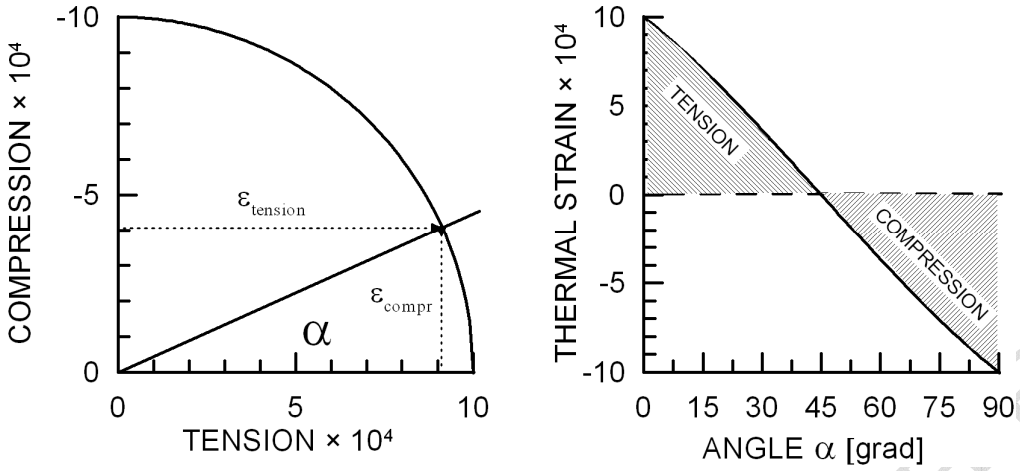

a) b)

Fig. 7 - Rudajevova

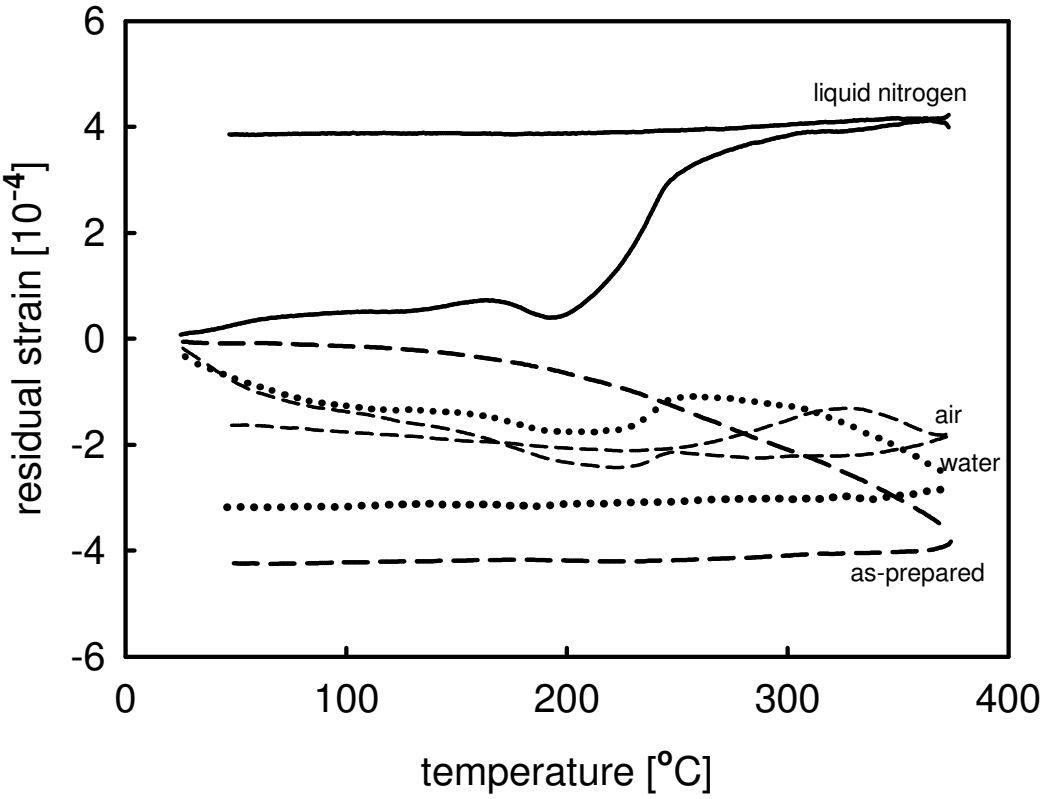

331 Fig. 8 - Rudajevova
332